THE PENNSYLVANIA STATE UNIVERSITY
SCHREYER HONORS COLLEGE

Characterization and Astrocyte-Specific Knockout of Acyl-CoA-Binding Protein Using a Cre-LoxP Model

CARLEY MYKUT
SPRING 2026

A thesis
submitted in partial fulfillment
of the requirements
for a baccalaureate degree
in Biology
with honors in Biology

Reviewed and approved* by the following:

Grayson Sipe
Assistant Professor of Biology
Thesis Supervisor

Benoît Dayrat
Associate Professor of Biology
Thesis Honors Adviser

* Electronic approvals are on file.

ABSTRACT

Post-traumatic stress disorder (PTSD) is a complex neuropsychiatric condition characterized by anxiety and the disarray of many other neuronal mechanisms. While most research is focused on neurons, astrocytes are an emerging area for many researchers. One astrocyte-specific protein, Acyl-CoA-binding protein (ACBP), which is also known as diazepam binding inhibitor (DBI), has been linked to stress and anxiety regulation.

Within this study, we evaluated the effectiveness of an inducible Cre-recombinase system for astrocyte-specific knockout and characterized its distribution across brain regions and cell types. Adult transgenic mice expressing Aldh1l1-CreERT2 were crossed with floxed DBI mice and administered tamoxifen to induce recombination. Brain tissue from the primary motor cortex (M1), caudate & putamen (CPu), and hippocampus (CA1) was analyzed using immunohistochemistry and confocal analysis to quantify DBI expression in astrocytes, neurons, and microglia.

Results demonstrated a significant difference in DBI expression in astrocytes for Cre+ animals compared to control animals (Cre^-) ($p < 0.05$). This confirmed the specificity of the Lox/P model for astrocytes. Furthermore, no significant changes in DBI expression for neurons and microglia were present. Likewise, further regional analysis revealed the ubiquitous nature of the DBI protein across brain regions studied: M1, CPu, and CA1.

These findings validate the inducible Cre/LoxP system utilized to be astrocyte specific. This model now provides a foundation for further behavioral studies investigating the role of astrocyte-specific DBI expression in stress and anxiety regulation.

TABLE OF CONTENTS

LIST OF FIGURES

LIST OF TABLES

ACKNOWLEDGEMENTS

This work represents the culmination of years of support and continuous learning as well as support from many individuals who have contributed to my growth as a researcher. I am grateful to everyone who helped make this project possible.

I would like to begin by thanking my thesis advisor, Dr. Sipe, for giving me the opportunity to join his lab and for fostering an environment that encouraged curiosity and community. His guidance has played a huge role in shaping this project, and I greatly appreciate the trust he placed in me throughout this process.

I would also like to extend my gratitude to Yuting Bai, my lab manager, for her support and assistance throughout this project. Her knowledge and willingness to help made a meaningful difference in the day-to-day progress of this work. Her joyful spirit lifted me through the hardest days and allowed me to step into lab and view the space as a breath of fresh air.

I am also grateful to my honors adviser, Dr. Benoît Dayrat, for taking the time to review this thesis and provide thoughtful feedback and insight.

Finally, I would like to thank my family and friends for their constant encouragement and support.

Chapter 1

INTRODUCTION

Post-traumatic stress disorder (PTSD) is a debilitating neurological disorder characterized by persistent adverse changes in arousal, mood, and cognition long after exposure to acute traumatic events. Throughout life, individuals can experience a wide range of traumatic events including sexual assault, stalking, unexpected death, combat exposure, and more life-threatening situations; according to an epidemiology study, roughly 70% of people encounter a trauma in their life and, on average, each person is exposed to about three traumas per lifetime (Kessler et al., 2017). After a traumatic incident, onset of PTSD symptoms can develop including debilitating anxiety, vivid trauma re-experiences, arousal, avoidant tendencies, and more. These symptoms can drastically change, increasing and decreasing in frequency and severity, over a 12-month post-trauma period (ODonnell et al., 2007). Like most mental disorders, there is great PTSD heterogeneity within symptom presentation, disease progression, and even response to therapeutic interventions. Some symptoms may be more prevalent in some individuals than others and can vary across time, complicating diagnosis and treatment options (Zoellner et al., 2013). Likewise, certain neurological and environmental factors can influence the likelihood of developing PSTD and the severity of symptoms including sex, prior mental health conditions, geographical location, and personality traits (Jaksic et al., 2012; Perrin et al., 2014; Koenen et al., 2017). Considering both characteristics above, PTSD is an increasingly difficult disorder to diagnose due to the diverse symptom presentation and different individual responses to traumatic events.

At the neurological level, PTSD and anxiety are not well understood and underlying mechanisms are debated among researchers. Yet, there is consensus that PTSD is related to dysregulation of fear-conditioning and stress responses, including the brain regions associated with these systems. Core brain regions implicated in these processes include the amygdala, which mediates fear processing –the hippocampus, which is involved in memory– and the prefrontal cortex, which regulates emotional responses and extinction of learning. Classic Pavlovian conditioning and behavioral responses to fearful situations are crucial to understanding where this pathway goes awry in PTSD presentation (Maeng et al., 2017; Abdallah et al., 2019).

Along with fear, stress also contributes greatly to PTSD and anxiety; therefore, it is worthwhile to understand how the mechanisms that regulate physiological and pathophysiological stress. Following the initial release of epinephrine and presentation of the "fight or flight" response, the secondary stress response is mediated by the hypothalamic–pituitary–adrenal (HPA) axis, which helps restore physiological homeostasis. Activation of the HPA axis begins with stimulation of neurons in the paraventricular nucleus, leading to the release of corticotropin-releasing hormone (CRH) and arginine vasopressin (AVP). These hormones act on the anterior pituitary gland to secrete cortisol, which then exerts negative feedback on the hypothalamus and pituitary, reducing further hormone release and facilitating the return to a baseline physiological state (Chu et al., 2017; Maeng et al., 2017). The intersection of fear and stress neuroactivity leads to research emphasis in the behavioral expression of anxiety and trauma responses. While there is much literature regarding neuronal

activity and overall brain structure pathophysiology, gaps in information and understanding are still prevalent and suggest an incomplete understanding in PTSD.

Most preclinical studies of PTSD in animal models have focused on neuronal physiology, while non-neuronal cells, such as astrocytes, have been largely understudied. Astrocytes bidirectionally communicate with neuronal networks and are integral to synaptic plasticity, which is a key process that transfers acute traumatic responses to the long-term negative symptoms of PTSD (Murphy-Royal et al., 2020). Likewise, through the reuptake of K^+, astrocytes are thought to improve the signal-to-noise ratio of neuronal encoding and modulate global states throughout the brain. This evidence suggest that astrocytes can control the excitability and inhibition of neuronal networks and modulate behavior (Wang et al., 2012).

In particular, some studies suggest that astrocytes are crucial in stress response within the central nervous system (CNS) and dysfunction can lead to neurological dysfunction. Changes in mood and increased stress can have a dramatic effect on astrocytes including altering gene expression, density, and morphology (Murphy-Royal et al., 2019). One example of morphology dysfunction was presented in a study by Lu et al. (2022), demonstrating that reducing expression, or the complete absence, of an astrocytic glucocorticoid receptor (GR) increased depressive-like behavior, suggesting that astrocytes play a role in mediating mood and anxiety-like behaviors especially through the glucocorticoid pathway. This same study also found that GRs in astrocytes were much more sensitive to stress than neuronal GRs.

Astrocytes are linked to many other bioactive factors that are tied to stress and anxiety phenotypes, which are prominent symptoms of PTSD. One such factor is Acyl-CoA-binding

protein (ACBP), which is also referred to as ‘diazepam binding inhibitor’ in the brain, because it competes with the benzodiazepine, diazepam, for binding sites on GABA receptors ($GABA_ARs$). GABA is the major inhibitory neurotransmitter in the CNS, and $GABA_ARs$ are ionotropic heteropentamers which allow the flow of chloride ions into neurons to hyperpolarize the cell and decrease overall cellular excitability on fast timescales (Ghit et al., 2021). Benzodiazepines (BZDs) are a widely prescribed and utilized drug class to combat stress and anxiety, as well as seizures. BZDs cross the blood-brain barrier after ingestion and have sedative effects on the CNS through interactions with $GABA_ARs$ (Edinoff, 2021). Due to ACBPs role in competitively interacting with benzodiazepines at $GABA_ARs$, it has been postulated that ACBP is an endogenous benzodiazepine (i.e., endozepine) that can modulate balances in excitation and inhibition. Although ACBP has many functions across the body, in the brain, ACBP is commonly referred to as diazepam binding inhibitor (DBI) and is highly expressed in astrocytes, particularly in the hypothalamus (Bouyakdan et al., 2015). Through similar studies, ACBP/DBI knockout mice have been found to have differential affects across brain regions, yet also a heightened impact on $GABA_ARs$ in the hippocampus. Further research suggested that DBI knockouts influence spatial learning and memory, normally hippocampal-driven tasks (Ujjainwala et al., 2019).

Since ACBP/DBI is found to act as an endogenous benzodiazepine, which mediates stress and anxiety, researchers have also studied the role of ACBP/DBI in anxiety phenotypes, particularly in astrocytes. One study used knockout (KO) $ACBP^{GFAP}$ mice to observe the neurological and behavioral changes. As ACBP is knocked out in this experiment, the hypothesis would be that anxiety-like tendencies would increase without the expression of the endozepine;

however, the experiment predicted a decrease in anxiety-like behaviors as they predicted no internal competition from ACBP for diazepam when administered. Once the KO was confirmed and diazepam was dispensed, the researchers tested the anxiety-like behaviors using open field (OF) and elevated plus maze (EPM). In conclusion, there was no difference in anxiety-like behaviors for male and female subjects. Although GFAP was used as an astrocyte marker, its expression in some non-astrocyte cells may explain the lack of differences in anxiety-like behaviors (Budry et al., 2016).

In conclusion, astrocyte-associated biomarkers such as ACBP/DBI suggest a pathway through which neuronal signaling and anxiety-related behaviors may be regulated. Recent findings suggest areas for improvement in isolating ACBP astrocyte function and diving into the understanding of endozepine function both in physiological and pathophysiological conditions. To address this, my thesis will characterize cell-type expression of ACBP/DBI in the normal mouse brain and verify astrocyte specific knockout of ACBP selectively using a Cre/LoxP transgenic model to observe the neurobiological changes; this study lays the foundation for future experiments examining the physiological and behavioral consequences of astrocyte-specific ACBP/DBI loss of function.

Chapter 2

MATERIALS AND METHODS

Animals

Experimental procedures were conducted in accordance with National Institutes of Health animal care guidelines and received approval from the Pennsylvania State University Institutional Animal Care and Use Committee. An inducible astrocyte-specific Cre recombinase mouse line (e.g., Aldh1l1-CreERT2) was crossed with a mouse line that has the ACBP/DBI gene surrounded by LoxP sites (i.e., flox-DBI). These animals underwent genomic testing to determine if they exhibited the floxed-DBI gene mutation or not. All test subjects were adult mice (14-16 weeks of age) housed on a reverse 12-hour light/dark cycle. Subjects were also given access to quality food and water throughout the duration of the experiment.

Polymerase Chain Reaction

Genomic DNA was extracted from animal ear tissue samples and then incubated in a lysis buffer within a labeled Eppendorf tube. Samples were incubated at 95 °C for 1-hour and then mechanically disturbed and broken up to release more DNA while being neutralized by a solution. Polymerase Chain Reaction (PCR) was performed to amplify targeted genomic regions. Reactions were prepared in 10 µL units and run under a standard PCR reaction. Products of PCR were visualized via gel electrophoresis (1.5 g agarose gel in 100 mL TAE). Gel was run for 20-30 minutes, or until bands were ¾ way down the agarose. DNA bands were visualized using a UV transilluminator and imaged for analysis. The presence or absence of bands determined

genotype. Experimental groups in this research were Cre^{+}/DBI f^{+}/f^{+} and control were Cre^{+}/DBI f^{+}/wt.

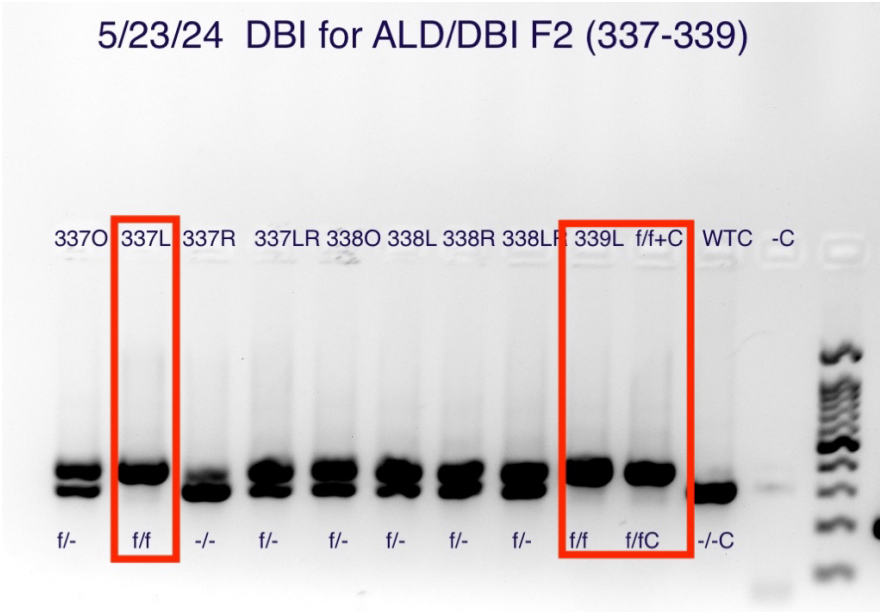

Figure 1. PCR for ALD/DBI Cross.

Tamoxifen Injections

Tamoxifen was utilized within the experiment to induce excision of the target gene via induced Cre-LoxP sites. Due to the selective nature of our target gene in one location– astrocytes –within the transgenic mouse line, this method was necessary to allow Cre to enter the nucleus and excise the gene in adult mice to avoid developmental confounds. Cre recombinase is selective to astrocytes but requires tamoxifen to become active and travel from the cytoplasm to the nucleus, leading to gene recombination. Tamoxifen (Sigma-Aldrich) was prepared at 20 mg/mL in corn oil by shaking overnight at 37 °C in a light-protected container, in this case aluminum foil, and stored at 4 °C for the duration of use. Adult mice received intraperitoneal injections of tamoxifen at approximately 75 mg/kg body weight (typically 100 µL per mouse)

once every 24 hours for five consecutive days, following an Institutional Animal Care and Use Committee–approved protocol. Injection sites were sanitized with 70% ethanol prior to administration. After the final injection, mice were quarantined for 24 hours before being returned to standard housing, and animals were monitored throughout treatment and post-injection periods for any adverse effects.

Perfusion & Vibratome

After 2-weeks and 4-weeks post-completion of tamoxifen injections, animals were anesthetized using isoflurane and were transcardially perfused to dissect the brain. Tissue was then placed into 4% formaldehyde for 24-hours and then placed into 0.1 M phosphate buffered solution (PBS) for long-term storage at 4 °C. Brain tissue was then sliced coronally (50 µm section thickness) using a vibratome and oscillating razor blade. Tissue was removed from storage, dried, and mounted onto a plate using an adhesive, with the posterior end secured to the plate. This tissue was then placed within the vibratome within 0.1 M PBS and slicing commenced. Each slice was serially collected into a 24-well plate and were submerged in 0.1 M PBS and sodium azide (1:1000) for preservation. The 24-well plates were then wrapped with Parafilm for further conservation and stored at 4 °C until further immunohistochemical processing.

Immunohistochemistry

Free-floating brain slices housed in 0.1 M PBS and diluted sodium azide were used, and specific tissue slices were selected to undergo immunohistochemistry (IHC) staining. Sections

were chosen to sample diverse brain regions; 4-5 slices were then placed into another 24-well plate filled with 0.1 M PBS to ensure proper and even staining across all tissues utilized. All solution volumes and antibody dilutions used below were adjusted based on well size and number of samples.

On Day 1 on IHC, tissue was washed 3 x 10 minutes on an orbital shaker at medium speed at room temperature. Between each wash, wells had their 0.1 M PBS (phosphate-buffered solution) washed and replaced with fresh solution. After this was completed, slices were then placed in a blocking solution to ensure non-specific binding does not occur further in the IHC process. Each well was incubated with 400 µL 0.1 M PBS, 500 µL 5% BSA, and 100 µL 1% Triton X-100. This incubation period lasted 1-hour on a medium-speed orbital shaker at room temperature. Once this period ended, the tissue was placed directly into the primary antibody solution without any additional washes. The primary antibody comprised the same agents as the blocking solution, yet in slightly different quantities per well: 344 µL PBS, 150 µL BSA, 5 µL of Triton, and roughly 1 µL of 1° antibody. See Table 1. below for detailed antibody selection and concentration. The tissue was incubated with the primary antibody solution at 4 °C on an orbital shaker overnight.

On Day 2 of IHC, sections were taken out of the orbital shaker and washed once again 3 x 10 minutes. This was then followed by incubation of the 2° antibody solution for 3-hours on a shaker at room temperature. Subsequent washes (3 × 10 minutes in 0.1 M PBS) were performed before mounting sections onto glass slides with anti-fade DAPI mounting media. Coverslips were applied and the slides were then sealed with nail polish for preservation. These slides were then placed in a light-protected container at 4 °C until ready for confocal analysis. Below are the specific stains used throughout the experiment:

Table 1. Antibody Selection and Concentrations DBI Characterization: IHC

	1° antibody	Concentration	2° antibody	Concentration
Stain #1	Rb α-DBI Chk α-S100beta	1:1000 1:500	α-Rbt (488 nm) α-Chk (594 nm)	1:500 1:500
Stain #2	Rb α-DBI GP α-Iba1	1:1000 1:500	α-Rbt (488 nm) α-GP (594 nm)	1:500 1:500
Stain #3	Rb α-DBI Ms α-Olig2	1:1000 1:500	α-Rbt (488 nm) α-Ms (594 nm)	1:500 1:500
Stain #4	Rb α-DBI GP α-NeuN	1:1000 1:500	α-Rbt (488 nm) α-GP (594 nm)	1:500 1:500

Confocal Imaging

Slices were imaged using a confocal scanning microscope. Slides were placed on the stage and the 20x air immersion objective was used. The layers, or phases, of the dye detectors were organized in a way that would minimize spectral overlap; these phases were organized by two channels. Each scan had the consistent parameters of 5.0 % laser power and 500 photon-multiplier tube (PMT) voltage, while ensuring the signal is not oversaturated or with excessive background noise. A three-dimensional construction was performed via Z-stack acquisition.

Image Analysis

Manual quantification of cell populations and co-localization was performed using FIJI (ImageJ). Images were converted to a uniform 500 x 500-pixel z-stack. Brightness was adjusted to a common format across all slides. Cells were manually counted across all three channels using the multi-point tool. Colocalization was determined via overlap of channel intensity and confirmed with DAPI staining for nuclei. These counts were further analyzed using averages and standard deviation for statistical analysis.

Chapter 3

RESULTS

Table 2. Cohort design for analysis

Mouse Line	Treatment Group	Sample Size	Brain Regions Assessed	IHC Target Cell Markers
Cre^{+}/DBI f^{+}/f^{+}	2-weeks post Tamoxifen injection	n= 2	M1, CPu, CA1	Astrocytes (S100B), Microglia (Iba1), Oligodendrocytes (Olig2), Neurons (NeuN)
Cre^{+}/DBI f^{+}/f^{+}	4-weeks post Tamoxifen injection	n= 3	M1, CPu, CA1	Astrocytes (S100B), Microglia (Iba1), Oligodendrocytes (Olig2), Neurons (NeuN)
DBI f^{+}/f^{+}	2-weeks post Tamoxifen injection	n= 2	M1, CPu, CA1	Astrocytes (S100B), Microglia (Iba1), Oligodendrocytes (Olig2), Neurons (NeuN)
DBI f^{+}/f^{+}	4-weeks post Tamoxifen injection	n= 2	M1, CPu, CA1	Astrocytes (S100B), Microglia (Iba1), Oligodendrocytes (Olig2), Neurons (NeuN)

As mentioned, for all analyses, data were collected and presented with standard error of the mean, $\pm\, SEM,$ *$p < 0.05$. For all analyses, 2-week and 4-week cohorts were combined for a larger sample size for each. Across all cohorts, DBI expression was measured in various site across the brain including the primary motor cortex (M1), caudate and putamen (CPu), and hippocampus (CA1). Likewise, multiple cell types were also analyzed including astrocytes, neurons, and microglia.

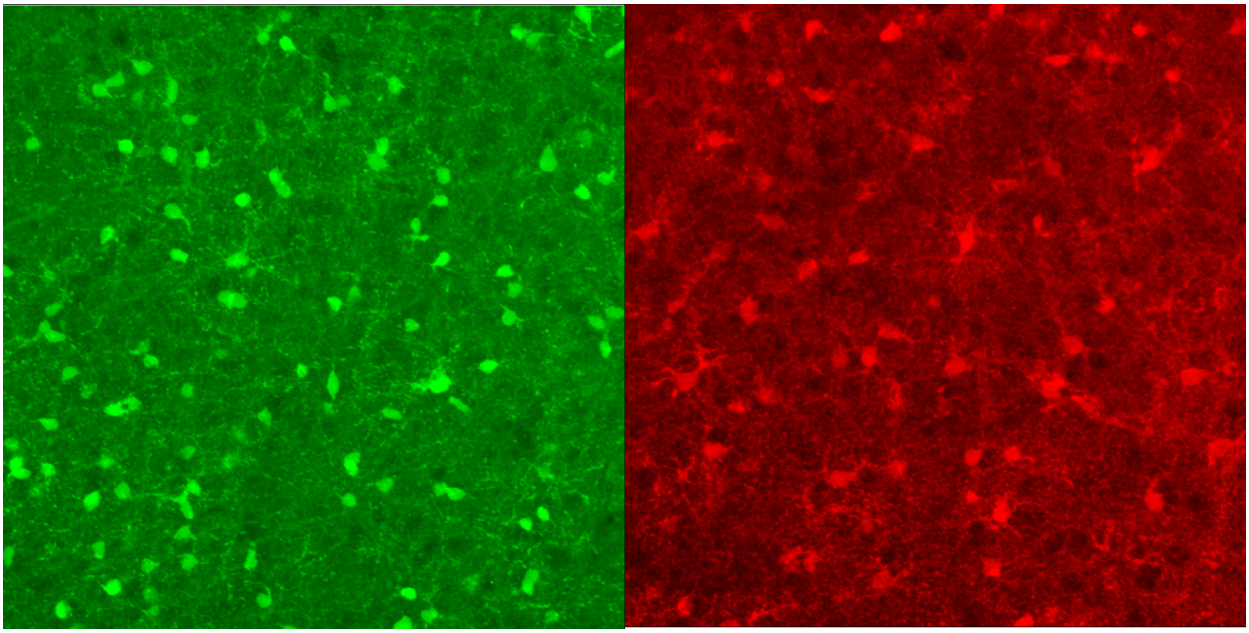

Figure 2. Sample image of Animal 298L (Cre^{+}) motor cortex (M1) for Stain #1. Channel #1 (green) highlights DBI-expressing cells and channel #2 (red) highlights astrocytes.

Representative imaging (Figure 2) confirms labeling of DBI-expressing cells and astrocytes, demonstrating patterns in fluorescence and successful IHC. The staining was able to produce clear images to analyze ACBP/DBI expression across different cell types in brain areas sampled. The figure above highlights DBI-expressing cells (green) in channel #1 and S100β (red) in channel #2. Not shown was channel #3, which stained nuclei with DAPI to confirm individual cells. These 500 x 500-pixel units were labeled, counted, and then overlayed with each other to observe possible colocalization. For both DBI-expressing cells and astrocytes, the cells are equally expressed and spread throughout the cortical layer. The morphology of both the astrocytes and DBI-expressing cells is consistent with what was expected. These images are representative of all other data collected via confocal imaging that were then analyzed with the statistical analysis described in the methods and materials section.

Table 3. Comparison of DBI expression in Cre^+ (n=3) and Cre^- (n=3) cells across the brain for major brain cell types (astrocytes, neurons, and microglia), including total counts, average expression levels, and statistical significance assessed ($p < 0.05$).

	# Cre^+ cells expressing DBI	**# Cre^- cells expressing DBI**	**Avg. Cre^+ cells expressing DBI**	**Avg. Cre^- cells expressing DBI**	**Chi-Squared p-value**
Astrocyte	23	197	1.53	16.42	*0.0341
Neuron	21	17	1.4	1.42	0.1144
Microglia	0	1	0	0.08	1

Table 3., compares the quantity of DBI-expression in Cre^+ and Cre^- cells across the brain (in all cell types: astrocytes, neurons, and microglia). Each subject was stained and analyzed for how many specific cell types, DBI-expressing cells, and colocalized with cell type & DBI-expressing cells. Above details the total number of Cre^+ & Cre^- cells expressing DBI in each cell type. This analysis was meant to demonstrate whether the KO was successful. Since the KO was specific to astrocytes, there is expected to be a reduction, or resulting in no astrocytes expressing DBI in Cre^+ subjects. In Cre^- cells, astrocytes should continue to express DBI and have a higher rate of colocalization than other cell types. On the other hand, for other cell types (neurons and microglia) there should not be a difference in expression of DBI for Cre^+ and Cre^- cells. Demonstrated in Table 3. is also an average number of DBI-expressing cells in Cre^+ and Cre^- cells per sample. When observing the results, astrocytes exhibited the most pronounced change, with Cre^- animals showing substantially higher total DBI-expressing cell counts (197 vs. 23) and a higher average number of DBI^+ cells per sample (16.42 vs. 1.53). This difference was statistically significant ($p = 0.0341$), indicating that Cre-mediated recombination is associated

with a significant reduction of DBI-expression in astrocytes, which was the goal of this experiment. Likewise, the sheer magnitude of this change suggests that astrocytes represent the main cell population affected by the DBI-KO model.

a)

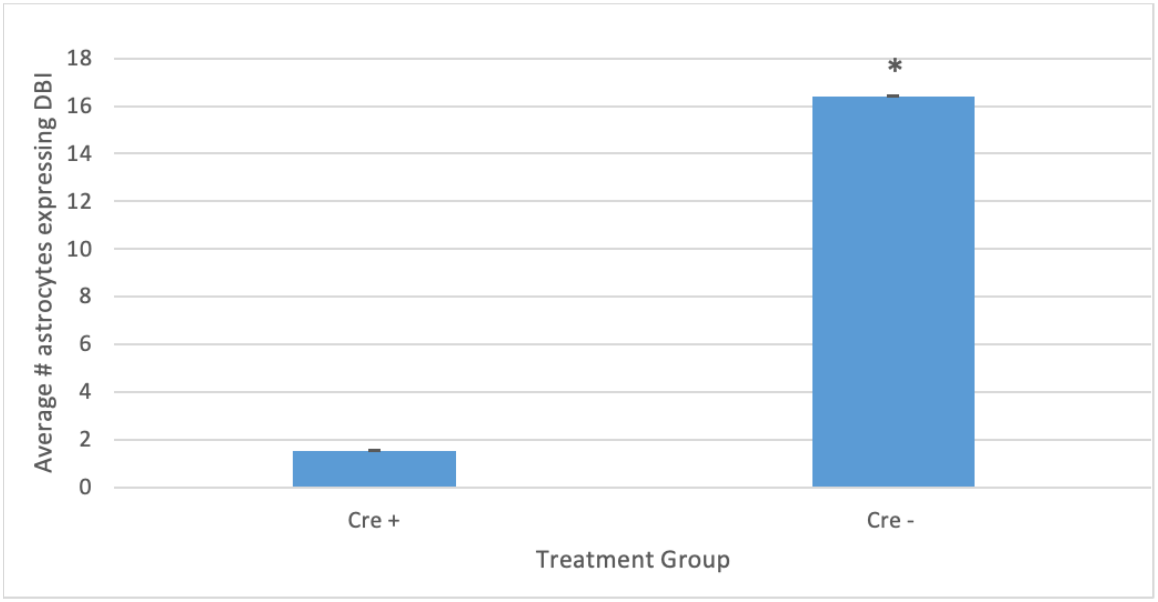

b)

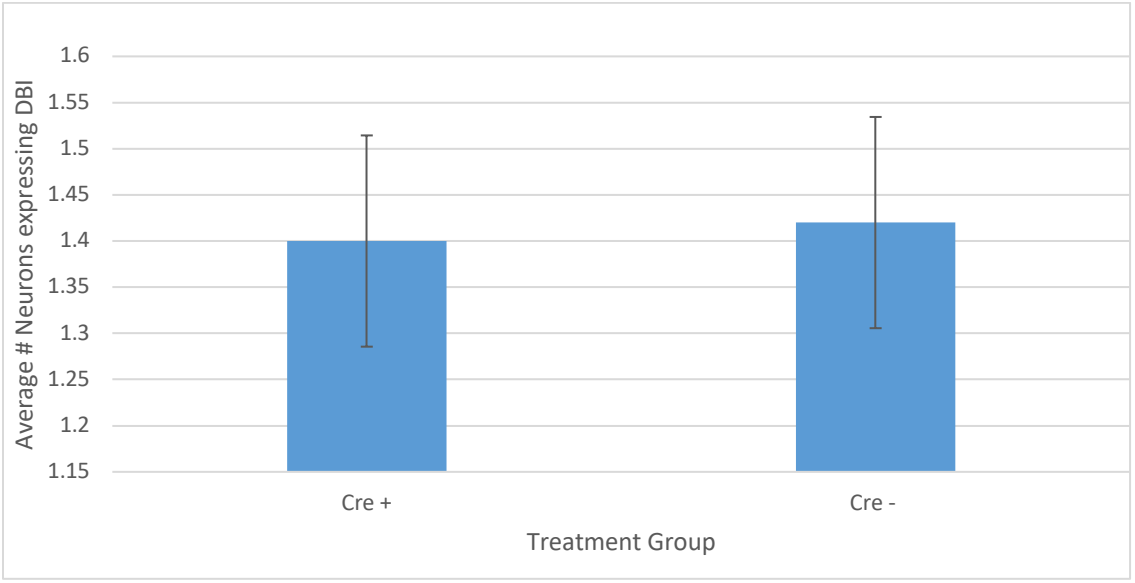

c)

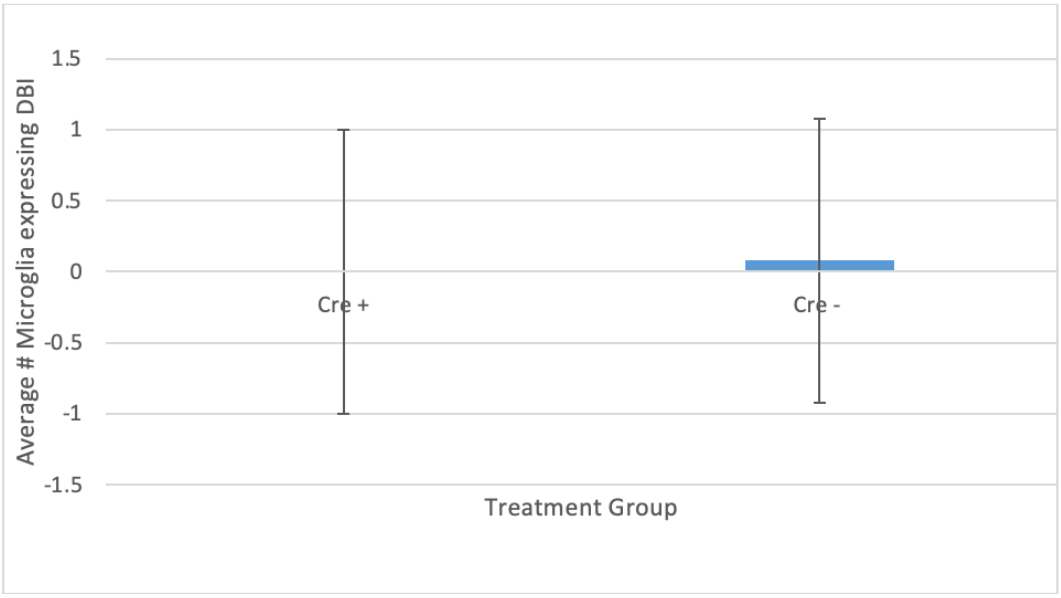

Figure 3. DBI expression across cell types in Cre^+ and Cre^- groups. **(a)** Astrocytes **(b)** Neurons **(c)** Microglia. Bars represent mean values, and error bars indicate variability via standard error. Asterisk (*) denotes statistical significance ($p < 0.05$).

In contrast, the neuronal DBI-expression was relatively low, compared to astrocytes, and had similar counts between Cre^+ and Cre^- experimental groups (21 vs. 17), respectively. Likewise, nearly identical average DBI^+ cells per sample (1.40 vs. 1.42). These two groups demonstrated a lack of statistical significance ($p=0.1144$). This result contributes to the success of the Cre-recombinase KO, since Cre-ERT2 is not a biomarker expressed commonly by neurons. Neurons were not affected substantially, or much at all, by being Cre^+. This suggests limited baseline DBI expression in neurons.

Microglia were similar and expressed minimal DBI overall, with only a single cell expressing DBI with a Cre^- subject and zero microglia expressing DBI in the Cre^+ experimental group. Average expression values were negligible (0 vs. 0.08), and no statistical significance was observed ($p = 1$).

Error bars (± SEM) for astrocytes further highlight the consistency of reduced DBI-expression in the Cre^{+} group, and the relatively small variation in neuronal and microglial data reflects their overall low contribution to DBI-expression.

Table 4. Quantification of DBI expression in Cre^{-} astrocytes across brain regions.

	# Cre^{-} astrocytes w/ DBI	Total astrocytes	% Cre^{-} astrocytes expressing DBI
M1	60	193	31.1%
CPu	37	143	25.9%
CA1	85	223	38.1%

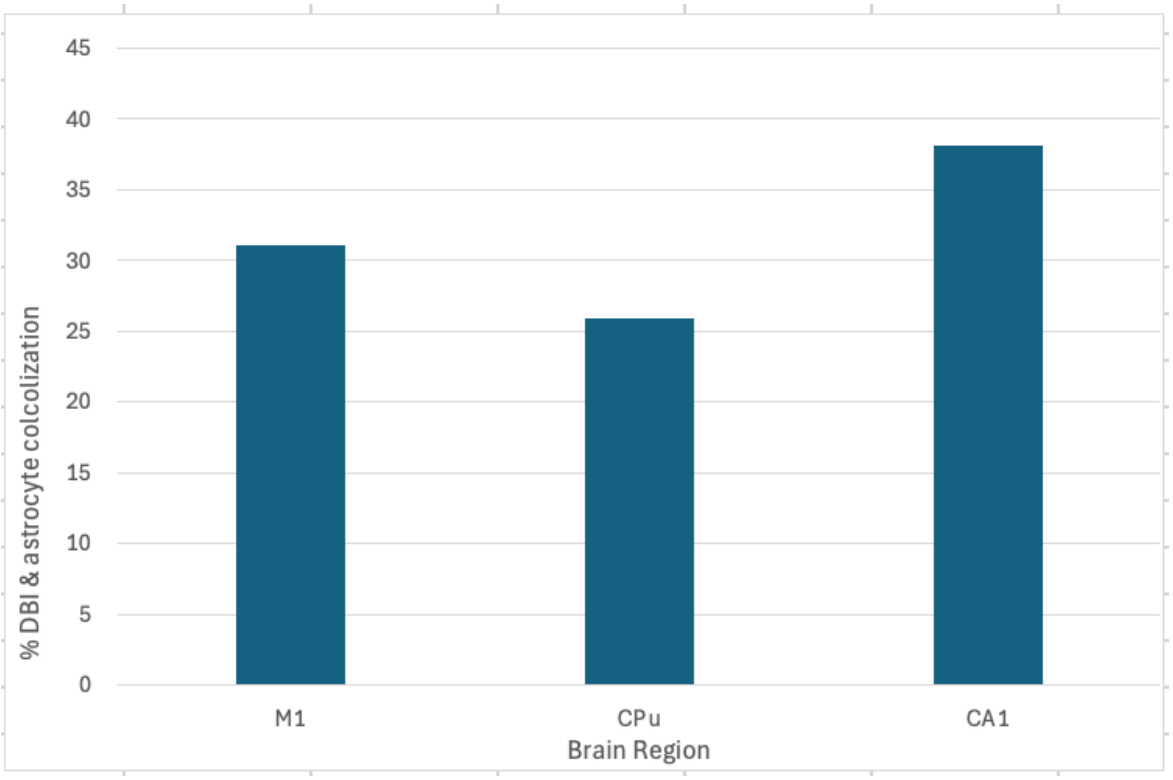

Figure 4. Percent (%) DBI & astrocyte colocalization in Cre^{-} subjects at each brain region.

Although the Cre-recombinases' effect on DBI-expression was the main part of the experiment above, other conclusions can also be found looking at the Cre- control group. For example, regional variability for the production of DBI-expressing astrocytes. Within this analysis and presented on Table 4., we observed the studied regions: M1, CPu, and CA1. Among these three brain regions, CA1, or the hippocampus, exhibited the highest percentage at 38.1% of astrocytes expressing DBI. Following CA1, was the motor cortex, or M1, which presented 31.1% of astrocytes expressing DBI. And finally, the caudate and putamen exhibited 25.9% of astrocytes expressing DBI. This presents a small pattern of increased DBI expression within astrocytes in the hippocampus CA1 region relative to other areas studied.

Although there are some differences regionally, there was consistent DBI-expression across all astrocytes in the regions analyzed. Figure 4. demonstrates these findings visually with the percent of DBI/astrocyte colocalization in Cre^- subjects at each brain region.

Chapter 4

DISCUSSION

My thesis above was presented to evaluate the effectiveness of a Cre-mediated DBI knockout (KO) model, specifically targeted for astrocytes. To observe the expression patterns of DBI throughout various cell types and brain regions. Overall, the results demonstrate a successful and specific knockout of DBI in astrocytes for subjects that are Cre^{+}, with minimal off-target effect for neurons and microglia. Additionally, DBI-expression is predominantly localized to astrocytes, with a reduction in DBI-expression for the Cre^{+} cell population.

The most significant finding of this thesis is that Cre-ERT2 LoxP model was effective and can now be utilized in future studies, specifically for neurophysiological and behavioral experiments. When looking at the astrocyte expression in Cre^{+} and Cre^{-} animals, there was a substantial reduction in DBI^{+} astrocytes and average DBI expression per sample in the Cre^{+} group with an achieved p-value of 0.05. This supports the effectiveness of the Cre-ERT2 system in selectively targeting astrocytes, confirming that the DBI knockout was successfully induced in the intended cell type. One Hu et al. (2020) study, concluded that Cre-mediated recombinase was most effective in specificity when driven by Aldh1l1-CreERT2 compared to five other astrocyte specific promoters. This was the transgenic line that was utilized within this experiment and therefore demonstrates the validity of this model in the field of transgenic mouse lines for inducible Cre-recombinase. There should be some attention drawn to the fact that some DBI were still present in astrocytes after the inducible Cre system was implemented. Some cells, a small subset, still presented DBI within astrocytes even after the tamoxifen injection occurred. In the same study, Hu et al. (2020), mentioned that Aldh1l1-CreERT2 may have a slightly lower efficiency and may miss various astrocyte subgroups, which could explain the small amount of

leakage. This partial resistance is not uncommon yet should be taken in account when completing further behavioral experiments.

Adding to the success of the model was the lack of reduction of DBI-expression in neurons and microglia. When observing these two groups, the sample counts and average expression per sample remained low and unchanged from Cre^+ to Cre^-. This lack of significance demonstrated the specificity of the Aldh1l1-Cre-ERT2, specific to astrocytes. This aligns with the assumption that the Aldh1l1 promoter is unique to astrocytes and not present in subsets of other cell types.

Beyond confirming the success of the knockout model, this thesis also was able to look at other areas of analysis. Although the knockout model was the main goal, within the Cre^- control group, we were able to examine where DBI-expression is the highest amongst a couple of brain regions including the primary motor cortex, caudate and putamen, and hippocampus. Analysis of the Cre^- animals revealed that DBI expression varies uniformly across brain regions. The highest proportion of DBI^+ astrocytes was observed in the CA1 region of the hippocampus, followed by the motor cortex, and then the caudate and putamen. DBI has not been well studied specifically in astrocytes, but this finding may provide more context on the broader signaling of the protein and its distributed functions across brain regions This may point future studies in looking more into DBI's role in region-specific modulation of neural activity or even local astrocyte-neuron signaling.

Although there were some statistically significant findings, there are several limitations that should be considered here. To start, the sample size across experimental groups were on the smaller end (n=2-3) per condition, which can influence statistical power and generalizability of results. Although combining the 2-week and 4-week cohorts increased the sample size, this was

not ideal due to the difference in experimental treatment for these two groups. The temporal effect of the induced Cre-recombinase, although peaks after 2-weeks, could have impacted the DBI-expression dynamics (Hu et al., 2020). Future studies should include larger sample sizes to strengthen the model's validity.

One area that was drawn to my attention after the conclusion of the study is that other cells are still expressing DBI. When analyzing the data, there were still some DBI^+ cells that were not astrocytes, neurons, or microglia. Although ACBP has many functions across the body, it is highly expressed in astrocytes, which is still a true statement after this study (Bouyakdan et al., 2015). However, there must be other cell types that express DBI within the brain, like oligodendrocytes, or DBI may be housed in non-cellular regions, such as the extracellular matrix. This could present itself to be a future study and may expose gaps in our understanding of this $GABA_ARs$ inhibitor.

Furthering our understanding of these DBI knockout animals could include performing behavioral assays like open field (OF) and elevated plus maze (EPM) utilized in the Budry et al. (2016) study. This would allow researchers to analyze the anxiety-related behaviors in these mice. Within the small scope of DBI research, there is still some contention present of whether a DBI knockout would increase or decrease anxiety-like behavior. For some, like the Budry study above, it is believed that knocking out this endogenous diazepine would decrease anxiety. The rationale here is that this would allow for the release of competitive inhibition, and therefore increase more diazepam being able to bind in this study. However, within the role of an endogenous diazepine, the function here is to mimic diazepam and produce similar effects. So, subsequently, some researchers also argue that knocking-out DBI would increase anxiety behaviors. Therefore, additional studies integrating behavioral assays and other analyses will be

necessary to fully understand the effect of DBI on anxiety-like behaviors and resolve the competing hypotheses above.

Chapter 5

CONCLUSION

In conclusion, this thesis demonstrates that DBI expression is primarily associated with astrocytes and that Cre-mediated recombinase effectively reduces this expression in this cell type, without significantly affecting neurons and microglia. Furthermore, regional similarities in expression provide context that DBI is a regionally ubiquitous protein within the brain, suggesting wide-spread involvement in neural-circuits. The knockout utilized within this study was proven to be effective and could be continued to be utilized in further behavioral experiments; this would contribute to our understanding of the effect of DBI on anxiety-like behaviors and neural circuit regulation.

REFERENCES

Bouyakdan, K., Taïb, B., Budry, L., Zhao, S., Rodaros, D., Neess, D., Mandrup, S., Faergeman, N.J., & Alquier T. (2015). A novel role for central ACBP/DBI as a regulator of long-chain fatty acid metabolism in astrocytes. *Journal of Neurochemistry, 133*(2), 253-65. https://doi.org/10.1111/jnc.13035

Budry, L., Bouyakdan, K., Tobin, S., Rodaros, D., Marcher, A.-B., Mandrup, S., Fulton, S., & Alquier, T. (2016). DBI/ACBP loss-of-function does not affect anxiety-like behaviour but reduces anxiolytic responses to diazepam in mice. *Behavioural Brain Research, 313*, 201–207. https://doi.org/10.1016/j.bbr.2016.06.052

Edinoff, A. N., Nix, C. A., Hollier, J., Sagrera, C. E., Delacroix, B. M., Abubakar, T., Cornett, E. M., Kaye, A. M., & Kaye, A. D. (2021). Benzodiazepines: Uses, Dangers, and Clinical Considerations. *Neurology International*, *13*(4), 594-607. https://doi.org/10.3390/neurolint13040059

Ghit, A., Assal, D., Al-Shami, A. S., & Hussein, D. E. E. (2021). GABA_A receptors: Structure, function, pharmacology, and related disorders. *Journal of Genetic Engineering and Biotechnology*, *19*(1). https://doi.org/ 10.1186/s43141-021-00224-0

Hu, N. Y., Chen, Y. T., Wang, Q. Jie, W., Liu, Y. S., You, Q. L., Li, Z. L., Li, X. W., Reibel, S., Pfrieger, F. W., Yang, J.M., & Gao, T.-M. (2020). Expression Patterns of Inducible Cre Recombinase Driven by Differential Astrocyte-Specific Promoters in Transgenic Mouse Lines. *Neuroscience Buletin, 36,* 530–544. https://doi.org/10.1007/s12264-019-00451-z

Jakšić, N., Brajković, L., Ivezić, E., Topić, R., & Jakovljević, M. (2012). The role of personality traits in posttraumatic stress disorder (PTSD). *Psychiatria Danubina*, *24*(3), 256-66.

Kessler, R. C., Aguilar-Gaxiola, S., Alonso, J., Benjet, C., Bromet, E. J., Cardoso, G., Koenen, K. C. (2017). Trauma and PTSD in the WHO World Mental Health Surveys. *European Journal of Psychotraumatology*, *8*(5). https://doi.org/10.1080/20008198.2017.1353383

Koenen, K. C., Ratanatharathorn, A., Ng, L., McLaughlin, K. A., Bromet, E. J., Stein, D. J., Kessler, R. C. (2017). Posttraumatic stress disorder in the World Mental Health Surveys. *Psychological Medicine*, *47*(13), 2260–2274. https://doi.org/10.1017/S0033291717000708

Lu, C.-L., Ren, J., Mo, J. W., Fan, J., Guo, F., Chen, L. Y., Wen, Y. L., Li, S. J., Fang, Y. Y., Wu, Z. F., Li, Y. L., Gao, T. M., & Cao, X. (2022). Glucocorticoid receptor–dependent astrocytes mediate stress vulnerability. *Biological Psychiatry, 92*(3), 204–215. https://doi.org/10.1016/j.biopsych.2021.11.022

Maeng, L. Y. & Milad, M. R. (2017) Post-Traumatic Stress Disorder: The Relationship Between the Fear Response and Chronic Stress. *Chronic Stress*, *1*. https://doi.org/10.1177/2470547017713297

Murphy-Royal, C., Gordon, G. R., & Bains, J. S. (2019). Stress-induced structural and functional modifications of astrocytes—Further implicating glia in the central response to stress. *Glia, 67*, 1806–1820. https://doi.org/10.1002/glia.23610

Murphy-Royal, C., Johnston, A. D., Boyce, A. K. J., Diaz-Castro, B., Institoris, A., Peringod, G., Zhang, O., Stout, R. F., Spray, D. C., Thompson, R. J., Khakh, B. S., Bains, J. S., & Gordon, G. R. (2020). Stress gates an astrocytic energy reservoir to impair synaptic plasticity. *Nature Communications*, *11*. https://doi.org/10.1038/s41467-020-15778-9

O'Donnell, M. L., Elliott, P., Lau, W., & Creamer, M. (2007). PTSD symptom trajectories: From early to chronic response. *Behaviour Research and Therapy, 45*(3), 601–606. https://doi.org/10.1016/j.brat.2006.03.015

Perrin, M., Vandeleur, C. L., Castelao, E., Rothen, S., Glaus, J., Vollenweider, P., & Preisig, M. (2014). Determinants of the development of post-traumatic stress disorder in the general population. *Social Psychiatry and Psychiatric Epidemiology, 49*(3), 447–457. https://doi.org/10.1007/s00127-013-0762-3

Schincariol, A., Orrù, G., Otgaar, H., Sartori, G., & Scarpazza, C. (2024). Posttraumatic stress disorder (PTSD) prevalence: An umbrella review. *Psychological Medicine, 54*, 4021–4034. https://doi.org/10.1017/S0033291723004040

Ujjainwala, A. L., Courtney, C. D., Wojnowski, N. M., Rhodes, J. S., & Christian, C. A. (2019). Differential impacts on multiple forms of spatial and contextual memory in diazepam binding inhibitor knockout mice. *Journal of Neuroscience Research, 97*(6), 683–697. https://doi.org/10.1002/jnr.24393

Wang, F., Smith, N. A., Xu, Q., Fujita, T., Baba, A., Matsuda, T., Takano, T., Bekar, L., & Nedergaard, M. (2012). Astrocytes modulate neural network activity by Ca^{2+}-dependent uptake of extracellular K^{+}. *Science Signaling, 5*(26). https://doi.org/10.1126/scisignal.2002334

Zoellner, L. A., Pruitt, L. D., Farach, F. J., & Jun, J. J. (2014). Understanding heterogeneity in PTSD: Fear, dysphoria, and distress. *Depression and Anxiety, 31*(2), 97–106. https://doi.org/10.1002/da.22133